ORIGINAL ARTICLE

Molecular structure activity investigation and spectroscopic analysis on (4-Chloro-2-methylphenoxy) acetic acid using Computational methods

Susithra G, Ramalingam S, Periandy S, Aarthi R

Susithra G, Ramalingam S, Periandy S, et al. Molecular structure activity investigation and spectroscopic analysis on (4-Chloro-2-methylphenoxy) acetic acid using Computational methods. J Pharmacol Med Chem 2018;2(1):4-17.

ABSTRACT

The molecular and biological properties of 4-Chloro-2-methylphenoxy acetic acid constructed by addition of appropriate ligands on suitable place of phenoxy acidic acid have been sumptuously interpreted in this research work. The investigation made using experimental tools such as FT-IR, FT-Raman, NMR and UV-Visible spectroscopy and theoretical tool; HF and DFT quantum computations. The systematic analyses associated with molecular dynamic characteristics have been performed to explore unknown physico-chemical properties and applications. The dislocation of chemical shift of base and ligand group in downward and upward field according to the anisotropic chemical reaction was discussed deeply and the tailored chemical mechanism to induce physico-chemical properties was determined. The transformation of electro-chemical energy by inducing transitions among electronic degeneracy interaction orbitals was examined. The important CT-complex of the molecule was found and the transitions between NBMO have been inspected. The rule of 5 (RO5) was validated for the present compound. The QSAR properties were computed and accounted for describing biological activity. The drug activity was elucidated according to the regulator and controller of the ligand groups over base system. The reduced toxicity effect was evaluated and verified by simulating VCD spectrum.

Key words: *4-Chloro-2-methylphenoxy acetic acid; Anisotropic-chemical reaction; CT-complex; NBMO; QSAR; RO_5.*

The Phenoxyacetic acid is fundamentally aryloxyacetic acid which is mainly used for the treatment of high blood pressure and edema caused by diseases similar to congestive heart failure, liver failure, and kidney failure. The major function of this acid is to treat the hypertension. The further addition of chlorine and methyl group with Phenoxyacetic acid, is enabled the compound for the treatment of insulin resistance, and hyperglycemia (1-3). The Phenoxyacetic acid and its derivative; substituted with suitable ligands in appropriate positions (halogen in ortho and methyl group in para) phenoxyacetic acids have enriched biological properties (4). These acids are also used as herbicide and pesticide (5,6) formulations. The (4-Chloro-2-methylphenoxy) acetic acid is normally used as special compound for Antimicro-bioactivity. The directed phenoxy properties and controlled acidic content of the present compound has consistent anticancer, antitumor, analgesic and anti-inflammatory properties (7,8).

The 2,4,5-Phenoxy acetic acid was used to control competing vegetation so that planted seedlings could become established and grow to renew forests (9,10). The present substance also used in agriculture field to destroy plant pests (11). The structure modification by suitable electron donating and withdrawing ligands over phenoxy acidic acid is enriched the biological as well as antibiotic properties (12). Hence, up to now, after the careful viewing the literature, it is established that, no research work has been published to investigate the interpretation on the biological activity and structure relative properties on (4-Chloro-2-methylphenoxy) acetic acid using computational calculations and electronic structure analysis. In this present work, a detailed spectroscopic analysis, QSAR studies and NMBO examinations have been carried out.

METHODOLOGY

Experimental details

Physical state:

• The prepared compound; (4-Chloro-2-methylphenoxy) acetic acid has been taken in liquid form which is uncontaminated and spectroscopic grade for obtaining spectra.

Recording profile:

• The FT-IR and FT-Raman spectra have been recorded in Bruker IFS 66V spectrometer and the instrument adopted with an FRA 106 Raman module equipped with a Nd:YAG laser source operating at 1.064 μm line widths with 200 mW power (13).

• The well distinct 1HNMR and 13CNMR spectra were recorded using high resolution FT-NMR spectrometer with 400 MHz for 1H and 100 MHz for 13C (14) with TMS as internal standard.

• The UV-Vis spectrum was recorded in the range of 200 nm to 800 nm, Hitachi UV-3200 spectrophotometer (15).

Computational methodology: In order to analyse the experimental data, the theoretical calculations have been performed to examine the structural, spectral, Mulliken charge profile, Frontier molecular orbital interaction process and the participation of CT complex on the electronic structure using the Gaussian 09 D. 01 version, Software program in MAC 3 computer (16). The complicated computational process was executed by HF and DFT-B3LYP and B3PW91 methods adopted with 6-31++G (d, p) and 6-311++G(d,p) basis sets. The biological activity parameters and QSAR properties were calculated using HyperChem software module. The drug like parameters (Lipinski) were estimated and evaluated for the title compound.

The energy consumed intensity modulated IR, Raman and electronic spectra, NMBO display and Frontier energy transitions levels have been identified and estimated using time-dependent SCF method with suitable basis set. The 1H and 13C NMR spectra have been analyzed to predict chemical shifts on par with TMS by GIAO method using I-PCM model with suitable basis set. The multipole moment, chemical related parameters and chemical reactivity index were calculated from filled, unfilled and continuum energy levels. The hyper active strain was calculated from linear and nonlinear Polarizability in different internal coordinates were computed using B3LYP method with the 6-311++G (d,p) basis set. The VCD spectrum was computed from sequential absorption and scattering frequencies and the optical chirality pattern was discussed.

RESULTS AND DISCUSSION

Structural deformation analysis

Department of Physics, A.V.C. College, Mayiladuthurai, Tamil Nadu, India

Correspondence: Dr. S. Ramalingam, Department of Physics, A.V.C. College, Mayiladuthurai, Tamil Nadu, India. Telephone 04364222264, email ramalingam.physics@gmail.com

Received: February 24, 2018, Accepted: March 02, 2018, Published: March 29, 2018

The molecular structure of present compound belongs to CS point group symmetry since it was composed of methoxy acid chain, methyl and chlorine entity in different dimensional planes. The molecular structure is optimized by Berny's optimization algorithm with the help of internal coordinate system using Gaussian 09 and Gauss view program and is shown in Figure 1.

The comparative optimized structural parameters such as bond length, bond angle and dihedral angle are presented in Table 1. The present molecule contains acid group which is coupled through by methoxy assembly called Phenoxy acidic acid. The Phenoxy unit was also substituted by chlorine atom and methyl group.

TABLE 1

Optimized geometrical parameters for (4-Chloro-2-methylphenoxy) acetic acid computed at HF/DFT (B3LYP&B3PW91) with 6-31++G(d,p) and 6-311++G(d,p) basis sets

Geometrical Parameters	Methods		
	HF 6-311++G (d, p)	B3LYP 6-311++G (d,p)	B3PW91 6-311++G (d,p)
	Bond length(Å)		
C1-C2	1.37	1.384	1.383
C1-C6	1.388	1.393	1.392
C1-Cl 10	1.746	1.761	1.747
C2-C3	1.391	1.396	1.393
C2-C7	1.073	1.082	1.083
C3-C4	1.38	1.393	1.391
C3-H8	1.073	1.082	1.083
C4 -C5	1.399	1.407	1.405
C4-O11	1.356	1.375	1.368
C5-C6	1.379	1.392	1.389
C5-C19	1.507	1.505	1.5
C6-H9	1.074	1.083	1.084
O11-C12	1.386	1.408	1.402
C12-H13	1.082	1.093	1.094
C12-H14	1.083	1.093	1.094
C12-C15	1.518	1.526	1.521
C15-O16	1.182	1.204	1.203
C15--O17	1.317	1.344	1.338
O17-H18	0.946	0.969	0.968
C19-H20	1.085	1.093	1.094
C19-H21	1.083	1.091	1.091
	Bond angle (˚)		
C2-C1-C6	120.619	120.853	120.733
C2-C1-Cl10	120.018	119.777	119.837
C6-C1-CL10	119.362	119.369	119.429
C1-C2-C3	119.315	119.158	119.21
C1-C2-H7	120.652	120.589	120.513
C3-C2-H7	120.031	120.251	120.275
C2-C3-C4	120.151	120.133	120.165
C2-C3-H8	118.276	118.455	118.45
C4-C3-H8	121.572	121.4105	121.383
C3-C4 -C5	120.744	120.881	120.837
C3-C4-O11	124.154	124.202	124.196
C5-C4-O11	115.101	114.915	114.964
C4-C5-C6	118.279	118.1746	118.189
C4-C5-C19	120.248	120.295	120.219
C6-C5-C19	121.472	121.53	121.591
C1-C6-C5	120.89	120.7976	120.863
C1-C6-H9	119.409	119.641	119.594
C5-C6-H9	119.699	119.561	119.544
C4-O11-C12	120.797	119.252	118.779
O11-C12-H13	112.6868	112.5374	112.603
O11-C12-H14	106.2045	105.6992	105.871
O11-C12-C15	115.2773	115.9576	116.014
H13-C12-H14	107.9164	107.6836	107.482
H13-C12-C15	107.9474	107.8267	107.817
H14-C12-C15	106.3873	106.6771	106.565
C12-C15-O16	122.3391	122.6791	122.625
C12-C15-O17	113.8167	113.2687	113.259
O16-C15-O17	123.7898	124.0012	124.064
C15-O17-H18	108.9383	107.334	107.017

C5-C19-H20	110.9435	111.1327	111.107
C5-C19-H21	110.5236	110.7908	110.844
C5-C19-H22	110.8413	111.0125	110.985
H20-C19-H21	108.5252	108.4787	108.479
H20-C19-H22	107.2863	106.704	106.704
H21-C19-H22	108.6156	108.5818	108.58
	Dihedral angles (°)		
C6-C1-C2-C3	-0.077	-0.1109	-0.118
C6-C1-C2-H7	179.8363	179.7367	179.733
CL10-C1-C2-C3	-179.9883	-179.9724	-179.98
CL10-C1-C2-H7	-0.0749	-0.1247	-0.131
C2-C1-C6-C5	0.0902	0.1459	0.1558
C2-C1-C6-H9	-179.8916	-179.8326	-179.84
CL10-C1-C6-C5	-179.998	-179.9921	-179.98
CL10-C1-C6-H9	0.0202	0.0294	0.0285
C1-C2-C3-C4	-0.0717	-0.1173	-0.1157
C1-C2-C3-H8	179.8151	179.6215	179.592
H7-C2-C3-C4	-179.9856	-179.9655	-179.97
H7-C2-C3-H8	-0.0988	-0.2266	-0.259
C2-C3-C4-C5	0.2094	0.3145	0.3157
C2-C3-C4-O11	-179.6025	-179.4276	-179.42
H8-C3-C4-C5	-179.6736	-179.4165	-179.38
H8-C3-C4-O11	0.5146	0.8414	0.8813
C3-C4-C5-C6	-0.1941	-0.2765	-0.275
C3-C4-C5-C19	179.721	179.6534	179.653
O11-C4-C5-C6	179.634	179.4884	179.483
O11-C4-C5-C19	-0.4509	-0.5817	-0.5884
C3-C4-O11-C12	0.7	0.2967	0.6159
C5-C4-O11-C12	-179.1215	-179.4593	-179.13
C4-C5-C6-C1	0.045	0.0476	0.0406
C4-C5-C6-H9	-179.9733	-179.9739	-179.97
C1-C5-C6-C1	-179.869	-179.8814	-179.89
C19-C5-C6-C9)	0.1127	0.0971	0.1053
C4,C5-C19-H20	59.9875	60.176	60.1221
C4-C5-C19-H21	-179.5794	-179.145	-179.18
C4-C5-C19-H22	-59.1	-58.4162	-58.435
C6-C5-C19-H20	-120.1003	-119.8965	-119.95
C6-C5-C19-H21	0.3329	0.7825	0.7467
C6-C5-C19-H22	120.8123	121.5113	121.49
C4-O11-C12-H13	49.8247	49.9897	50.2523
C4-O11-C12-H14	167.7752	167.2646	167.423
C4-O11-C12-C15	-74.6995	-74.8065	-74.635
O11-C12-C15-O16	158.7889	162.2186	162.717
O11-C12-C15-O17	-23.8008	-20.2838	-19.804
H13-C12-C15-O16	31.8257	35.0372	35.4119
H13-C12-C15-O17	-150.764	-147.4653	-147.11
H14-C12-C15-O16	-83.7885	-80.3942	-79.726
H14-C12-C15-O17	93.6218	97.1034	97.7538
C12-C15-O17-H18	-178.6478	-178.8292	-178.96
O16-C15-O17-H18	-1.2806	-1.3699	-1.5265

Usually, the ligand addition is surely making impact on ring and thereby can be observed in compression and elongation of bond length and angle. Due to the chain injection, the ring was found to be heavily stressed and the strain was formed at the midpoint of chain and methyl group which was clearly seen in the expansion of bond length C4-C5 (1.407Å). The bond length of C1-C2 was 1.384 Å which was identified to be compressed since the chlorine only was placed at that point of ring. The bond length C4-C5, C1-C6, C3-C4 and C2-C3 were almost equal and rather difference was found between them since such bond lengths were associated with ligand substitution point. The bond length of C-O at acid group was 1.344 Å whereas the C-O between methoxy and ring were 1.408 and 1.375 Å respectively. From this variation, it was clear that, the bond length was found to be stretched much in methoxy when compared with acid group. In order to compensate the chemical repulsive forces existed between O and C of ring, the bond was stretched out.

Normally, the inner angle of each semicircle of the hexagonal ring is 120°, whenever the substitutions added to the hexagonal ring, the angles are changed according to the mass of the substitutions. If the change of angle greater than 120° the fundamental property of the hexagonal ring will be vanished and the change of property will be according to the substitutions. In this case, the bond angle C4-C5-C6 was appeared to be compressed 118.17° which was very less when compared with other semicircle angles of the ring. This view showed the distortion of hexagonal structure which described the distortion of basic property of the ring and existence of new property.

Mulliken charge analysis

Normally, the charge distributed configuration of aromatic system displayed chemical energy orientation due to the chemical interactive process taking place by the addition of ligands in suitable position of the base ring. Such polarized charged system sponsored the chemical activity for producing biological and pharmaceutical properties (17). Usually, the Mulliken charge

level diagram configure electron cloud wherever need for generating desired drug property.

Here, the Mulliken charge level arrangements was displayed in the Figure 2 where the spreading of decisive stack point of electron clouds for oscillating the chemical potential to attain antibiotic characteristics. In the case of chain, the entire charges moved towards the ring from acid group with respect to O and it was evidenced by the appearance of darkness over O (neutral atom). Similarly, the green color of Cl showed that, the electron density displaced from Cl to ring. Whereas in the case of methyl group, the charge level was found to be retained in order to control the charge gradient on the ring. The absorbed negative gradient of charge were stagnated trigonally on C2, C4 and C6 of ring which is mainly for generating strong distinct dipoles for stabilizing chemical activity. The strong dipole was also found between C of methyl group and C of ring which is mostly for regulating and controlling chemical attractive potential.

From this arrangement of molecular charge intensity, it was clear that, the necessary electronic content of energy was moved from OCH2COOH chain and Cl to the hexagonal ring, which created the asymmetric charge equilibrium and it was controlled and regulated by methyl group on head of the ring. This view of wide dispersal charge entities in the compound produced antibiotic nature.

Molecular properties, Lipinski "Rule of five" and Bioactivity score

The of Lipinski's and drug-like parameters of title compound were calculated by HyperChem 8.0.6 software and were depicted in Table 2. The results of bio activity parameters were calculated using Molinspiration online database. The simulated topographical polar surface area and calculated lipophilicity diagrams of present compound were revealed in Figure 3.

The Rule of five or RO5 describes molecular properties important for a drug's pharmacokinetics in the human body, including their absorption, distribution, metabolism, and excretion (17). It is used to estimate drug likeness and if an aromatic chemical compound to be orally active drug in humans, it should have certain pharmacological or biological activity (18). The drug pharmacokinetics predicted that, the drug compound has poor absorption or permeation is more possible when there are more than 5 H-bond donors, 10 H-bond acceptors, the rotatable bonds is less than 10, the molecular weight (MWT) is greater than 500 and the calculated Log P (CLogP) is greater than 5 (or MlogP>4.15). But, in this case, the H-bond donor, acceptor and rotatable bonds were calculated to be 1, 3 and 3 respectively. The MWT and Log P were 200.62 Da. and 2.29 respectively. These values emphasized that, the present drug is suitable for oral formulations. In general, if the molecule contains total polar surface area ≤ 140 A^2, the compound has metabolic stability and transporter effects (19,20). Here, the TPSA was observed to be 46.5 A2. So, the present compound possessed better water-solubility and structure-based drug ability.

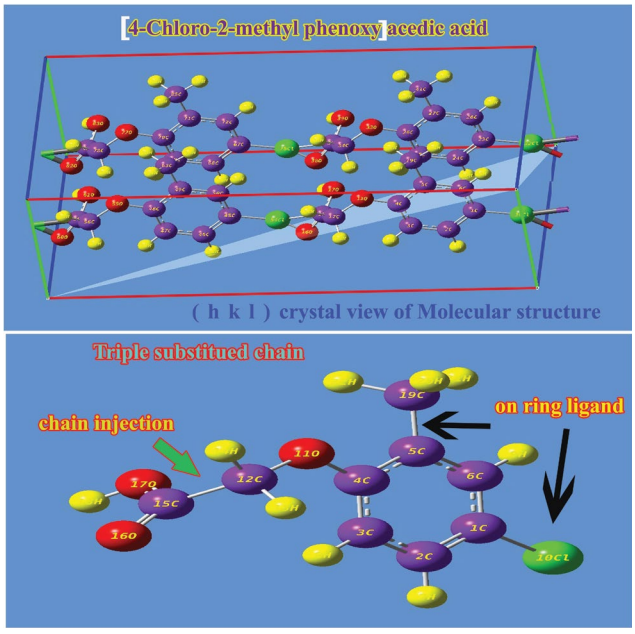

Figure 1) *Molecular structure of (4-Chloro-2-methylphenoxy) acetic acid*

In the present covalently bonded complex aromatic system, the heavy atom count and Covalently-Bonded Unit Count were computed to be 13 and 1 respectively. These values stressed that, the covalent bond character was enhanced by the substitution effect and the heavy atom was found to be Cl and O which were at suitable positions for the modification of sub-structure for enrichment of antibiotic activity of title compound. The drug likeness score is the complex balance of structural properties and various pharmacophoric features. Such a score influence behavior of the aromatic system in living organism. The value is mainly used for reliable toxicity prediction and measuring physicochemical properties of aromatic compound directly or indirectly. The score was calculated in the range of -0.28 - -0.98 for this case. This parameter range was observed to be negative; it was found to be observed in satisfactory region and well agreed with the literature (21). This view of molecule designated the compound as a new drug candidate with high transport quality. Based on the obtained results, the present drug was largely free of toxic effects.

The GPCR is G protein-coupled receptors (GPCRs) most diverse group of membrane receptors and it transmits signals from these substances to an intracellular molecule called a G protein. The GPCRs play precise role in activate inside signal transduction pathways and it offered useful targets for drug development. The transmitted signal value was identified to be -0.64 which was observed within the expected limit and this compound could be identified by cellular responses. The ion channel modulator value was determined to be -0.54 which was good enough and it is able to transport

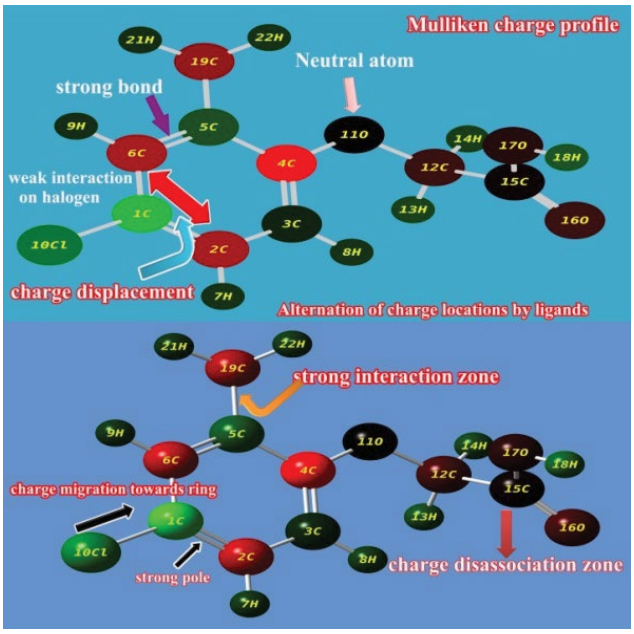

Figure 2) *Mulliken charge distribution of 4-Chloro-2-methylphenoxy) acetic acid*

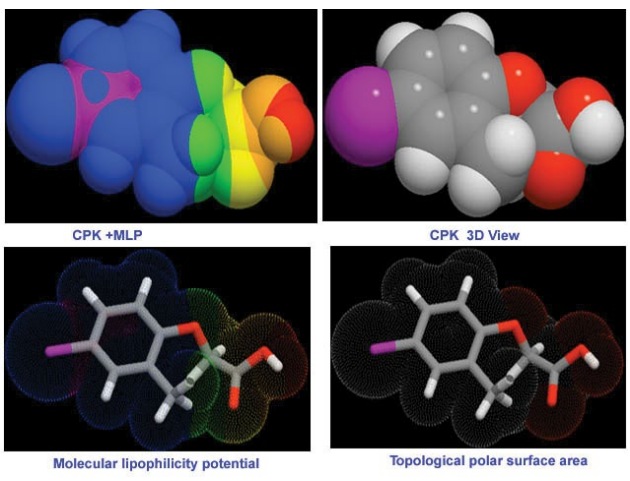

Figure 3) *Topographical view of 4-Chloro-2-methylphenoxy) acetic acid*

TABLE 2

Biological and structural parameters of (4-Chloro-2-methylphenoxy) acetic acid

Parameters	Values
Hydrogen bond donor count	1
Hydrogen bond acceptor	3
RotaTABLE bond count	3
Topological Polar Surface	46.5A^2
Mono isotopic Mass	200.024 g/mol
Exact Mass	200.024 g/mol
Heavy Atom Count	13
Covalently-Bonded Unit	1
n atoms	13
MW	200.62 Da
n ON	3
n OHNH	1
n violation	0
n rotb	3
volume	166.93
Mi logP	2.29
TPSA	46.53
GPCR Ligand	-0.64
Ion channel modulator	-0.54
Kinase inhibitor	-1.06
Nuclear receptor ligand	-0.26
Protease inhibitor	-0.94
Enzyme inhibitor	-0.36

ions (both anions and cations) across cell membranes to regulate various physiological processes and well agreed with the result obtained on work (22).

A protein kinase inhibitor is a kind of enzyme inhibitor which purposely blocks the action of protein kinases. Protein kinases are enzymes that add a phrosphate (PO) group to a protein or other organic molecule, usually on the serine, threonine, or tyrosine amino acid. The kinase inhibitor value was calculated to be 1.06 which was found to be above the threshold limit and able to modulate its function of protein kinases. The nuclear receptors are a special type of proteins identified within cells which is responsible for sensing steroid and thyroid hormones and useful for the embryonic development (23). The nuclear receptor value of present drug case was 0.26 and it is able to directly interact with and control the expression of genomic DNA. The Protease inhibitor is an antiviral quality of the chemical compound which was determined to be 0.94 and it was sufficient to prevent viral replication by selectively binding to viral proteases and blocking proteolytic cleavage of protein precursors.

Vibrational analysis

The vibrational assignments and their vibrational analysis of the chemical compound under study are an important study to find whether the compositional parts active or not. The activity of the molecular parts are to be examined according to their vibrational region of the spectrum since it play essential role in generating physico-chemical properties for providing compact drug activity. For that, the presence of various covalent dipoles and the corresponding fundamental characteristics region are to be identified. Here, the dipoles were addressed from realistic fundamental vibrational pattern and was obtained in Table 3. The thoroughly scanned FT-IR and FT-Raman vibrational frequencies of recorded and theoretical spectra were displayed in the Figures 4 and 5 respectively. The tailored molecule consists of the phenoxy acetic acid substituted by methyl and chlorine atoms. The final chemical product contains 22 atoms and its configuration fit in to CS point group. According to the selection rules of cyclic molecule, 60 wavenumbers of vibrations were disseminated. In total vibrational frequencies, 22 modes were recognized as stretching, 19 modes were represented as in plane bending and 19 peaks acknowledged as out of plane bending vibrations.

Γ Vibrations=41A′+19A″

All the vibrational modes were identified keenly and arranged according to their characteristic region. The active fundamentals were distinguished between IR and Raman frequencies in order according to the mutual exclusion principle. The entire bond lengths and bond angles were represented by normal mode of vibrations.

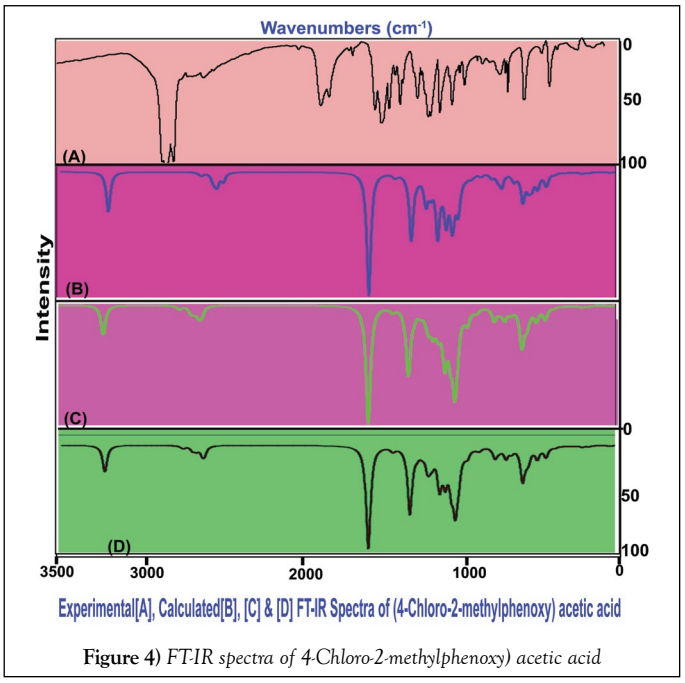

Figure 4) *FT-IR spectra of 4-Chloro-2-methylphenoxy) acetic acid*

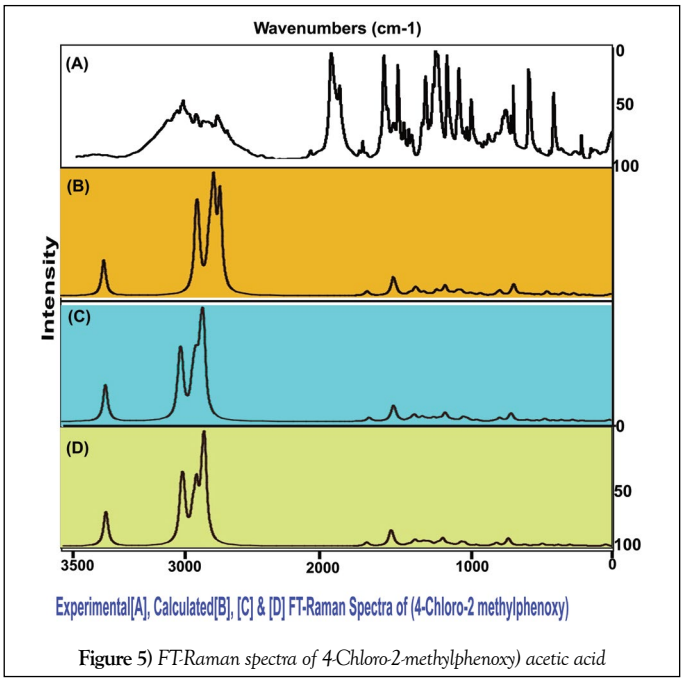

Figure 5) *FT-Raman spectra of 4-Chloro-2-methylphenoxy) acetic acid*

C-H vibrations

The present phenoxy derivative has basically benzene aromatic ring in which three substitutions have been identified. So the hexagonal ring having three remaining C-H bonds, according which, three C-H stretching modes was identified at 3060, 2970 and 2950 cm. Normally for the above said compounds, three bands with weak to medium intensity observed in the region 3100-3000 cm-1 due to C-H stretching vibrations (24,25). Here, one band was found in IR with strong intensity whereas two from Raman with weak intensity. As usual, these three modes are determined as pure stretching modes in which two of them hold back. This was mainly due to the absorption of ring energy by Cl.

The C-H in plane ring bending vibrations normally taking place with medium to weak intensity in the region 1300-1000 cm^{-1} (26). But, here, the peaks for C-H in plane bending vibrations were appeared with very strong to medium intensity at 1295, 1245 and 1240 cm-1. Usually, the C-H out of plane bending vibrations are observed in the region 950-780 cm^{-1} (27,28). In this case, these out of plane bending bands were found at 980, 950 and 890 cm^{-1}. Resembling to in plane bending, all the bands have been observed at the top end of the expected region. From this examination, it was clear that,

TABLE 3

Observed and HF and DFT (B3LYP & B3PW91) with 6-31++G(d,p) & 6-311++G (d,p) level calculated vibrational frequencies of (4-Chloro-2-methylphenoxy) acetic acid

S. No	Symmetry Species C_s	Observed frequency(cm^{-1})		Methods			Vibrational Assignments
		FT-IR	FT-Raman	HF 6-311++G (d,p)	B3LYP 6-311++G (d,p)	B3PW91 6-311++G (d,p)	
1	A′	3450w	-	3590	3567	3578	(O-H) υ
2	A′		3060w	2943	3049	3044	(C-H) υ
3	A′	2970s	2970w	2929	3035	3030	(C-H) υ
4	A′	-	2950w	2928	3033	3027	(C-H) υ
5	A′	2940s	2940w	2857	2958	2965	(C-H) υ
6	A′	2930s	-	2841	2943	2941	(C-H) υ
7	A′	-	2910w	2825	2929	2936	(C-H) υ
8	A′	2850s	-	2817	2900	2895	(C-H) υ
9	A′	2845s	-	2776	2882	2879	(C-H) υ
10	A′	1750vs	1750vs	1746	1722	1733	(C=O) υ
11	A′	1600w	1600m	1562	1553	1563	(C=C) υ
12	A′	1500vs	1500vs	1545	1539	1547	(C=C) υ
13	A′	-	1495vs	1445	1444	1443	(C=C) υ
14	A′	1490s	-	1411	1419	1410	(O-H) δ
15	A′	1460s	1460w	1407	1404	1391	(C-C) υ
16	A′	1450s	1450w	1396	1403	1390	(C-C) υ
17	A′	-	1430vs	1352	1357	1355	(C-C) υ
18	A′	1420s	-	1345	1348	1334	(C-O) υ
19	A′	1400w	1400m	1338	1319	1318	(C-O) υ
20	A′	1370s	-	1307	1300	1301	(C-O) υ
21	A″	-	1310vs	1258	1270	1284	(O-H) γ
22	A′	1295m	1295vs	1231	1239	1235	(C-H) δ
23	A′	-	1245vs	1199	1229	1221	(C-H) δ
24	A′	1240s	-	1156	1189	1195	(C-H) δ
25	A′	1230s	-	1143	1150	1153	(C-H) δ
26	A′	1190s	1190vs	1113	1121	1124	(C-H) δ
27	A′	1180s	-	1087	1104	1101	(C-H) δ
28	A′	1140s	-	1056	1062	1066	(C-H) δ
29	A′	-	1130vs	1023	1032	1040	(C-H) δ
30	A′	1080m	-	1016	1010	998	(C=O) δ
31	A′	-	1070s	999	984	976	(C-C) υ
32	A′	1030w	-	951	964	955	(C-C) υ
33	A′	-	980m	925	891	885	(C-H) γ
34	A″	950w	-	875	846	849	(C-H) γ
35	A″	890w	-	833	844	839	(C-H) γ
36	A″	880s	-	815	807	815	(C-H) γ
37	A″	-	870vs	805	774	770	(C-H) γ
38	A″	810s	-	718	728	732	(C-H) γ
39	A″	800s	800vs	704	695	691	(C-H) γ
40	A″	-	790vs	655	652	652	(C-H) γ
41	A′	680s	680vs	615	620	621	(C-Cl) υ
42	A′	650w	-	591	607	608	(CCC) δ
43	A′	610w	-	551	551	551	(CCC) δ
44	A′	580w	-	547	540	538	(CCC) δ
45	A′	560w	-	489	494	492	(C-O) δ

46	A′	550w	550w	483	489	488	(C-O) δ
47	A′	-	510w	431	433	430	(C-O) δ
48	A′	500w		428	428	425	(C-C) δ
49	A′	-	470w	373	376	378	(C-Cl) δ
50	A″	-	450w	345	338	339	(CCC) γ
51	A″	400w	-	296	297	296	(CCC) γ
52	A″	-	380w	239	239	238	(CCC) γ
53	A″	-	320w	224	227	224	(C-O) γ
54	A″	-	300w	190	192	192	(C-O) γ
55	A″	-	270w	186	184	185	(C-C) γ
56	A″	-	260w	137	125	122	(C-Cl) γ
57	A″	-	250w	107	106	106	(COOH) τ
58	A″	-	200w	51	51	51	(CH_3) τ
59	A″	-	150w	39	39	40	(OH) τ
60	A″	-	110w	29	34	35	(OCH_2) τ

VS: Very strong; S: Strong; m: Medium; w: Weak; as: Asymmetric; s: Symmetric; υ: Stretching; α: Deformation; δ: In Plane Bending; γ: Out Plane Bending; τ: Twisting

the C-H bending vibrations were found to be well within their limited array and it is also conclude that, energy of C-H bonds were affected in higher region than lower region.

C-C vibrations

Usually the static potential energy of core ring is directly related with the substitutions attached with it and also, it was fluctuated with respect to mass of ligand groups. Consequently, the vibrational region of core oscillations definitely affected and the corresponding modes disturbed the substitutional vibrations. Hence, the ring C=C and C-C stretching vibrations, known as semicircle stretching regularly happen in the region 1450-1650 cm^{-1} (29,30). In the present case, the C=C bonds can be identified on C1-C2, C3-C4 and C5-C6 clearly. Correspondingly, the stretching vibrations have been observed strongly at 1600, 1500 and 1495 cm^{-1}. The entire core CC stretching were found within the allowed region and well agreed with literature (31,32). Similarly, the C-C stretching vibrations were appeared at 1460, 1450 and 1430 cm^{-1}. When compared to the literature region mentioned over, there is rather decrement found in observed frequencies which is due to the causing of loading of heavy ligands with the ring. Most of the CC stretching bands were observed with very strong intensity and found in both IR and Raman spectra. In the present work, three semicircles CCC in plane breathing bands observed at 650, 610 and 580 cm^{-1} and three accompanying out of plane breathing bands were allotted at 450, 400 and 380 cm^{-1}. These assignments were found well below the expected region which was primarily due to the struggling of core potential energy by Cl and CH3 and agreed well with the literature (33).

Ethyl and methyl group vibrations

The present molecule contains ethylene group along with O and COOH in the chain. Generally, the C-H stretching vibrations of the methylene group are located at lower frequencies than those of the aromatic C-H ring stretching. The CH2 stretching vibration generally observed in the region 3000-2870 cm^{-1} (34,35). For this compound, the C-H stretching vibrations are observed with strong intensity at 2850 and 2845 cm^{-1}. By the void position of CH2, these stretching peaks have affected much. This indolent atmosphere showed partial energy exhaustion of CH2 by chain. Normally, the C-H scissoring mode is very active in ethylene substituted molecules (36). In the present assignment, the C-H scissoring bending modes are found with strong intensity at 1140 and 1130 cm 1 and the wagging modes determined with very strong intensity at 800 and 790 cm. These assignments validated the statement that, the part of bending energy was not affected which was rational with the literature report (37).

The title compound possesses a methyl group separately and their vibrational assignments certify the position of methyl group on top moiety of molecule. The asymmetric and the symmetric C-H symmetric vibrations in methyl group regularly determined in the region of 2990-2920 cm^{-1} and 2900-2840 cm^{-1} (38) respectively. In this case, the asymmetric C-H vibrations were occurring at 2940, 2930 and 2910 cm^{-1}. All those vibrations belong to asymmetric range and it was clear that, these modes were not affected by other vibrations. The in plane and out of plane bending vibrations were getting at 1230, 1190 and 1180 cm^{-1} and 880, 870 and 810 cm respectively. From the bending vibrations, it was clear that, the entire vibrations found exactly within the expected region and were not concealed much by the interaction of vinyl group.

Predicted by the DFT calculations, the compounds containing CH3 group, the series of the bands appearing as asymmetric and symmetric deformation modes in the region 1400-1500 cm^{-1} (34,39) are mainly due to methyl deformation, coupling with the C-H and C-C stretching frequencies, two different extends and in different way. In the present study, the Raman bands at 1460 cm^{-1} (very strong) and 1450 cm^{-1} (strong) are attributed to the asymmetric deformation modes of isopropyl group. Appearance of these bands is due to presence of two independent CH3 groups in the amino acid residues in different environments.

C-Cl vibrations

The present aromatic complex enclosed with Cl at Meta position and it was clearly demonstrated itself by its proportionate stretching and bending vibrations. In aromatic complex, the C-Cl stretching vibrations generally offered very strong bands in IR spectrum in the region of 760-505 cm^{-1} (40) due to its strong dipole moment. Accordingly, here, one peak was appeared with very strong intensity at 680 cm^{-1} for C-Cl stretching vibration. Most of the aromatic halogen-chlorine substituted compounds contain a band of strong to medium intensity in the region 385-265 cm^{-1} by C-Cl in-plane bending vibration (24). Hence, the IR band was identified at 470 cm−1 for C-Cl in-plane bending modes. The C-Cl out of plane deformation vibration was established at 260 cm^{-1}. The entire C-Cl vibrations are found within the expected region of the spectra which clearly showed that, the acidic nature was found to be regulated in this case. In addition to that, the acetic character was not dominated and its energy was rather consumed.

COOH vibrations

Normally, the acetic acids derivative is having strong C=O stretching strong band in the region 1600-1560 cm 1 and an additional strong band at 1230-1140 cm due to the stretching of the C-O bond (41). The stretching band linked with the σ- interaction bond; C-O is dependent on the nature of the acidic components. Although the acetic nature is less important, the Alkyl chloroformates have a very strong band due to the asymmetric COC stretching vibration at 1200-1130 cm-1, a strong band is also observed at 850-770 cm^{-1} (42). Usually, the Methyl esters of long-chain of aliphatic acid exhibit strong bands at 1175 cm^{-1}, 1250 cm^{-1} and 1205 cm^{-1} respectively. In, the primary acid; acetates possess a weak-intensity band at 1060-1035 cm^{-1} due to the asymmetric stretching of the O-CH2-C group. Hence, in this case, a very strong mode was observed at 1750 cm^{-1} due to C=O stretching vibration. It was occupied at the top of the crest due to its attaining of high force constant by absorbing chemical potential from associated atoms. The other three bands are with very strong to weak intensity recognized at 1420, 1400 and 1370 cm^{-1} for C-O stretching vibrations. Last one of these vibrational bands was assigned for acid group and other two vibrational modes were assigned for C-O bond which is located OCH_2 group. Here, irrespective of positions of C-O, the occurrence of the vibrational bands was found to be

elevated to well above the expected region. This elevated ambience of such peaks described the one way electrophilicity charge transition from ring to COOH group. The in plane and out of plane bending peaks were found at 560, 550 and 510 cm 1 and 320 and 300 cm. The entire bending vibrations were also elevated much and from which it was clear that, the charge cloud displacement is supported the energy of the bonds.

The hydroxyl bond related to acid group having stretching vibrations in the wavenumber region 3400-2500 cm^{-1} (43). The O-H group vibrations are possibly receptive in IR region since it has high value of force constant and shows prominent shifts in the spectra of the hydrogen bonded chemical species. Usually, O-H stretching frequency is observed with weak to medium intensity in the infrared spectrum and it is difficult to identify the exact position of peak since the spectra related OH is broad. In this case, the strong band come into view at 3450 cm^{-1} in the IR spectrum alone which was assigned to O-H stretching. The related O-H in-plane bending and out of plane vibrations are observed in the region 1440-1260 cm^{-1} and 517-710 cm^{-1} respectively. Accordingly, the observed in plane and out of plane bending vibrations of hydroxyl group were found at 1490 and 1310 cm^{-1} respectively. The COOH group twisting vibrations were determined at 250, 150 and 110 cm^{-1} in the far IR region. The entire OH vibrations significantly discussed and the locations of the peaks were keenly monitored. From this discussion, it was infer that, from the elevated vibrations, it was confirmed that, the chemical potential concentrated over COOH for generating enriched antibiotic property.

NMR assessment

The NMR technique is a great flexible tool which throwing innovative light on complex organic structure elucidation which is significantly used to find the chemical root path to produce dynamic chemical potential to induce desired molecular and biological property. It is also great tool for interpreting the constructed drug property and toxic effect. The 1H and 13C NMR spectra of present case were presented in Table 4. The experimental and calculated spectra are shown in Figure 5. The paramagnetic shield breaking and field spreading were also displayed in the Figure 6.

Usually, the rate of paramagnetic shield of electron concealed atom is broken by the surrounded atoms or molecules with it. The paramagnetic shield is very strong in the case of hexagonal ring unless the substitutions coupled with the ring. The rate of such shield breaking is directly depends on mass of the attached atoms or molecules which clearly explained the change of molecular property and thereby it is used to find the chemical nodal spot for producing biological and drug property. Usually, the shield breaking rate is measured by chemical shift in up and down field. In general, the range of 13C NMR chemical shifts for aromatic derivatives is greater or lesser than 100 ppm (44,45) is observed and the fluctuation regarding ligands used for the reliable interpretation of molecular property.

Here, the greater chemical shift (Expt. 152 and 174 ppm; Cal. 141 and 167 ppm) was found at C1 and C4 in which the Cl and acetic acid chain were substituted. The ring carbon C4 was more shifted than C1 since ligand chain with heavy mass was coupled with the ring. Due to the large chemical shift (>150 ppm), the C4 was noted as first chemical nodal point in which the considerable energy was exchanged from ring to chain. The chlorine coupled carbon was determined to be second nodal point in which the electronic energy was transferred to ring. The third nodal region was identified to be C5 in which the methyl ligand has been substituted and the chemical shift of 136 ppm was observed. The moderate chemical shift of 123, 133 and 134 were observed on C2, C3 and C6 respectively. The next higher chemical shift of 190 ppm was observed on acetic carbon C15 in which large amount of negative chemical potential was stored. The stored energy has been directed by the nodal points and controlled by methyl carbon which was confirmed by obtaining experimental and calculated chemical shift of 130 ppm and136 ppm respectively.

In the case of H on ring, the quite higher chemical shift was appeared than H on methyl and ethylene groups since the hydrogen linked with resonance hexagonal structure. The H8 was shifted more than other in the molecule since it was affected by asymmetrical interaction of electronegative species in the chain. From the observation, it was clear that, the charge cloud was moved disproportionately flow from methyl and chlorine to ring and ring to acetic acid ligand via nodal site of carbons in the ring. In this way, the exchange of electronic potential taking place between ring and ligands and generating consistent drug property such as antibiotic potential.

Frontier molecular interaction examination

Usually, the atomic orbital arrangement is modified as molecular configuration electronic system after the formation of aromatic complex and the interaction taking place between occupied and unoccupied molecular bands called HOMO and LUMO. In the molecular orbital pattern, many interaction entities are constructed with respect to degenerate energy system. During the energy transitions in the form electronic cloud transformation among such energy domains fabricating desired chemical environments for producing desired biological and drug property. The molecular orbital interface contour was shown in the Figure 7 and the energy profile value of orbital structure was depicting in the Table 5.

In order to prove the energy provenance of HOMO, the Π-bonding coupling appeared over the semicircle carbons C3=C4=C5 and C2=C1=C6 of ring which showed the crew of charge cloud with approximately equal energy called blended chemical energy. The bonded complex would produce resonance path for harmonic drift motion of charge cloud with similar characteristics. The Π-bond interaction system was found on Cl atom which also ready to supply energy by making transitions. The Π-bond overlapping scheme were also found on acetic acid ligand group particularly on O. The second order interaction arrangement of overlapping was observed on HOMO-1 which was enhanced completely and strongly. In ligand chain, there was no energy interaction found which ensured the exhaustion of charge interaction process for stabilizing generated property.

In LUMO, the π-bonding interaction become visible by which the carbons C3 and C4 of ring and O11, C12, C15, O16, O17 and H18 of chain were connected for creating empty potential zone for receiving electron cloud to form strong biological property. The negative iso surface of space interaction system was found between ring carbon and hydrogen of ethylene group which was due to accomplish the available overlapping orbital. In second lower empty interaction zone, there were number of individual Π and π-bonding matrix systems. This was mainly due to restrain chemical potential of receiving electron cloud from excited configuration zone.

From this interaction profile of FMP, it was conferred that, the π and δ

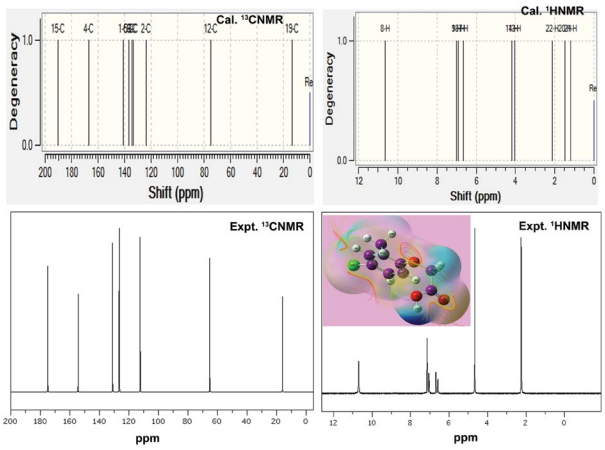

Figure 6) *13C and 1H NMR spectra of 4-Chloro-2-methylphenoxy) acetic acid*

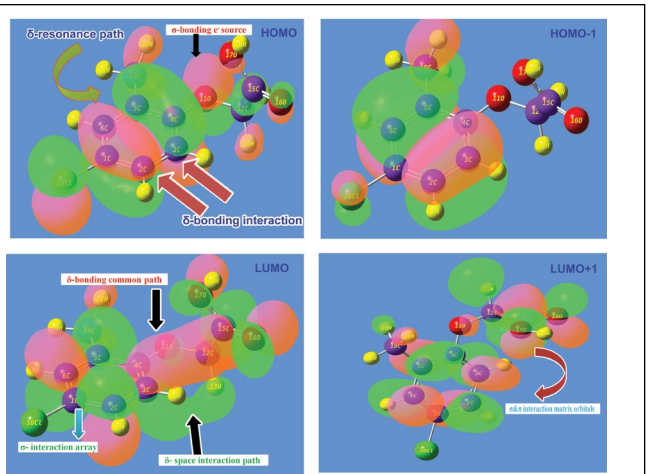

Figure 7) *Frontier molecular profile of 4-Chloro-2-methylphenoxy) acetic acid*

TABLE 4

Experimental and calculated 1H and 13C NMR chemical shifts of (4-Chloro-2-methylphenoxy) acetic acid

Atom position	TMS-B3LYP/6-311++G(2d,p)			Experimental shift (ppm)
	Gas	Solvent phase		
		DMSO	CCl_4	
C1	141.052	139.575	140.306	152
C2	123.532	123.732	123.574	125
C3	133.407	133.927	133.62	130
C4	167.038	167.419	167.265	174
C5	136.811	138.015	137.379	130
C6	134.613	134.739	134.656	130
C12	74.7178	75.4016	75.004	64
C15	190.46	192.46	191.448	-
C19	13.5986	13.4694	13.5448	15
H7	6.6621	6.7922	6.7156	6.5
H8	10.6255	10.5706	10.5951	10.7
H9	7.0086	7.1591	7.0708	7
H13	4.0496	4.1237	4.0878	4.7
H14	4.1774	4.4459	4.298	4.7
H18	6.9021	7.7197	7.2788	7.2
H20	1.4708	1.5607	1.5076	-
H21	1.1837	1.3572	1.2553	-
H22	2.1074	2.0231	2.0804	2.2

TABLE 5

Frontier molecular orbitals of (4-Chloro-2-methylphenoxy) acetic acid with energy level system

Energy levels	B3LYP/6-311++ G(d,p)	UV-Visible region
H+10	10.846	10.672
H+9	10.704	10.482
H+8	10.302	10.375
H+7	10.258	9.971
H+6	9.687	9.491
H+5	9.55	8.966
H+4	8.81	8.797
H+3	8.626	8.406
H+2	8.269	7.154
H+1	7.326	6.893
H	6.385	6.372
L	0.996	2.378
L-1	0.651	0.715
L-2	0.551	0.541
L-3	0.485	0.259
L-4	0.048	0.007
L-5	0.041	0.228
L-6	0.171	0.322
L-7	0.366	0.612
L-8	0.635	0.727
L-9	0.782	0.752
L-10	0.942	0.935

bonding interaction orbital domains available in ring and chain for the charge cloud orientation to drift chemical energy among intra molecular electronic entities to induce the strong chemical potential to persuade drug property. The energy transformation was restricted among HOMO and LUMO of present molecule by making degenerate interaction profile which was clearly seen in the Figure.

UV-Visible absorption CT complex profile

The electronic excited oscillations and UV-Visible absorption analytical factors of title molecule were presented in the Table 6 and related CT absorption profile diagram of both experimental and simulated were displayed in Figure 8. The determination of CT complex and the assignment of electronic absorption peak in UV-Visible characteristics spectra are very important. Because of it acquires the information regarding key factor to find the root cause of the drug property (46). The electronic spectra is usually represented by N=3 states which is applicable to analyze three oscillating transitions by which the UV-visible characteristics peaks are recognized. The signal contains three individual signals among which one or two peaks are identified with strong oscillator strength. Such a mode of absorption address the UV-Visible characterises and thereby the biological activity can be studied.

In this case, the base was phenoxy acetic acid and the methyl and chlorine species to be the ligands. According to the Mulliken analysis, such two substitutions (methyl and chlorine) were found to be regulator and controller of charge orientations between ring and acid group via methoxy groups. So the acid group along with methoxy impurity was found to be the CT complex of this aromatic complex system. The doubly excited peaks observed in the UV-Visible spectra was only due to the couple of n□ □ * transitions. These transitions were found at 403, 343 and 320 nm with the band gap of 3.071, 3.612 and 3.873 eV which were obtained strongly with oscillator strength of 0.001, 0.09 and 0.0017. The first band was located with very low oscillator strength in visible region whereas last two bands were identified with moderate strength in UV region. These have been found in gas phase while in solvent phase; DMSO and CCl4, all these absorption peaks were identified at same place with same band gap energies. Irrespective of gas and solvent phase, the entire absorption peaks were found between HOMO and LUMO set up and these transitions were belong to R-band.

The entire vibrational UV-Visible bands appraised that, the methoxy group along with acid group were recognized as ligand CT complex of present compound. This arrangement was found to be triggering the biological activity in the compound and thereby the antibiotic characteristics were achieved by addition of subordinate ligand groups (methyl and chlorine) in suitable positions.

Molecular electrostatic potential (MESP) maps assay

The electrostatic potential map display of the present molecule was portrayed in between two extreme potential and it's spreading of potential field contours shown in Figure 9. The extreme static potential gradient was limited in the region of ± 6.661 e-2. The positive and negative potentials were represented by the existence of arrangement of strong molecular dipoles i.e. net dipole moment of the molecule and are denoted by electrophilic and nucleophilic region. Such three dimensional region is constructed by spatial distribution of multipole moments grid points and this zone is normally covered the molecular orbital region also.

The 3D electrostatic potential on a molecular surface is primarily important because it is much more essential to explain the binding ability with associated protein and biological receptors (47). In this case, according to the Figure 9, the electron deficient zone was determined over the OH of COOH group labelled as nucleophilic cover and simultaneously, the electron rich zone was found at C=O of same group. This made asymmetrical strong dipole moment in the chain whereas electron fading region was found over hydrogen bond of the molecule. Normally, if the halogen is present in

TABLE 6

Theoretical electronic absorption spectra of (4-Chloro-2-methylphenoxy) acetic acid

λ (nm)	E (eV)	(*f*)	Transition levels	Major contribution	Assignment	Region	Bands
				Gas			
403.63	3.071	0.001	H→L(68%)		n→ σ*	Visible region	R-band
343.2	3.612	0.0192	H-2→L(54%)		n→ σ*	Quartz UV	
320.09	3.873	0.0017	H-1→L(55%)	H→L(68%)	n→ σ*	Quartz UV	(German,radikalartig)
				DMSO			
404.22	3.067	0.0001	H→L(68%)		n→ σ*	Visible region	R-band
343.48	3.609	0.0199	H-2→L(54%)	H→L(68%)	n→ σ*	Quartz UV	
320.5	3.868	0.0018	H-1→L(55%)		n→ σ*	Quartz UV	(German,radikalartig)
				CCl_4			
426.84	2.904	0.0002	H→L(68%)		n→ σ*	Visible region	R-band
351.68	3.525	0.0168			n→ σ*	Quartz UV	
334.78	3.703	0.0064	H-2→L(50%)	H→L(68%)	n→ σ*	Quartz UV	(German,radikalartig)

H: Homo; L: Lumo

TABLE 7

Calculated energies, chemical hardness, electro negativity, Chemical potential, Electrophilicity index of (4-Chloro-2-methylphenoxy) acetic acid

Parameter	B3LYP/ 6-311++G(d,p)	UV-Visible region
E_{total} (Hartree)	-1034.4457	-1034.0954
E_{HOMO} (eV)	6.3859	6.3726
E_{LUMO} (eV)	0.9967	2.378
$\Delta E_{OMO-\Lambda YMO\ \gamma\alpha\pi}$ (ες)	5.3892	3.9946
E_{HOMO-1} (eV)	7.3263	6.8937
E_{LUMO+1} (eV)	0.6511	0.7151
$\Delta E_{OMO-1-\Lambda YMO+1\ \gamma\alpha\pi}$ (ες)	6.6752	6.1786
Chemical hardness (h)	2.6946	1.9973
Electronegativity (χ)	3.6913	4.3753
Chemical potential (μ)	3.6913	4.3753
Chemical softness(S)	-10.7784	-7.9892
Electrophilicity index (ω)	2.5283	4.7922
Dipole moment	2.1094	4.879
ECT	2.1556	2.1533

molecule, the region around will be symbolized by electrophilic zone due to its rich electronegativity. But in this case, though the chlorine was substituted over ring, the region around was displayed to be electron deficient zone. This was obviously due to the asymmetrical displacement of electron cloud from Cl to ring for negative chemical potential on chain. The chemical potential field was originated on chain of the molecule and particularly, the negative potential valley concentrated over OCH2 group.

Physico-chemical properties

Usually, when the base is linked with ligand groups, the molecular orbital levels are re arranged with respect to the chemical equilibrium and the associated orbitals are splitted in to two bands. The physico-chemical residual is generally stored in the transitions among different energy levels of two bands of existed molecular orbital. The molecular structure and chemical properties are examined by determining associated parameters. The calculated important physical and chemical parameters were presented in the Table 7.

From the zero point vibrational energy of the present compound, the rate of optimization can be determined. Accordingly, these values in IR and UV-Visible region were found to be 1034.44 and 1034.09 Kcal/mol respectively. From these observed values, it was clear that, the molecular structure was optimized and it will provide the characteristics as it is. The dipole moment of the aromatics is usually measuring the charge spreading capacity and binding ability of the compound. Here, the molecular dipole moment was found as 2.10 and 4.87 dyne in IR and UV-visible region respectively. From this view, it was confer that, the structure was more stable in second region than first.

The chemical Hardness is most important parameter which is used to determine inertness against chemical flexibility and it measures the reaction capacity to unwanted sub ligands while processing. In phenoxy

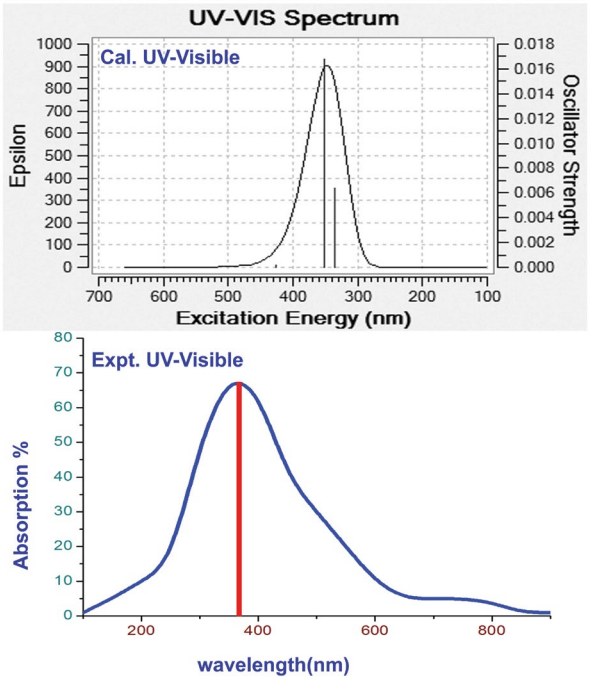

Figure 8) *UV-Visible spectra of 4-Chloro-2-methylphenoxy) acetic acid*

derivative, it was calculated to be 2.69 and 1.99 eV in IR and UV-Visible region respectively. The calculated values showed the chemical isolation ability to react with linked ligands. The ionization potential (IP) is mainly used for quantifying chemical bonds and it is also employed for the rate of electropositiveness (EP) of the chemical compounds. If the IP decreases, the EP increases much and reactiveness of the chemical species will be increased much. In this case, the IP was to be 0.99 and 2.37 eV in IR and UV-Visible respectively which were very low and the chemical reaction capacity was very high. The local electro-chemical steadiness of the chemical compounds can be assessed by the total electronegativity of a molecule under study which is a vital functional parameter used to predict electro-magnetic polarity of molecule (48). Here, it was determined to be 3.69 and 4.37 in IR and UV region respectively. The value of the same parameter was higher in UV-Visible than IR which was illustrated that, the entire compound was made by ionic bond instead of covalent bond.

The electrophilicity index is a novel chemical parameter that is utilized to evaluate the exchange of chemical potential energy flow through interactive molecular sites. Here, the electrophilicity index is 2.52 and 4.79 eV in IR and UV-Visible region respectively. In the UV-Visible region, it was found that, the hyper chemical potential flow was observed than IR since the present chemical compound was more reactive in UV-Visible than IR region. The ECT is a chemical property finding parameter and the main purpose of the factor is to determine the change of property of chemical species related to attach one. Here, the base is phenoxy acetic acid and its main drug application is the treatment of high blood pressure whereas when chlorine

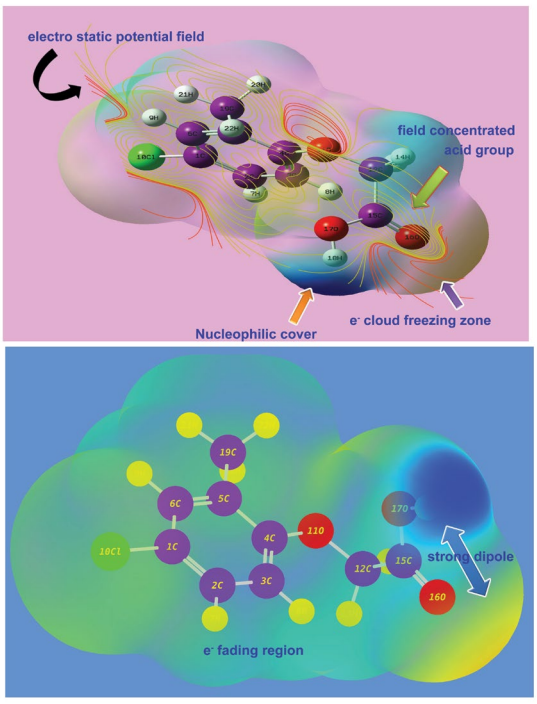

Figure 9) *MESP display of 4-Chloro-2-methylphenoxy) acetic acid*

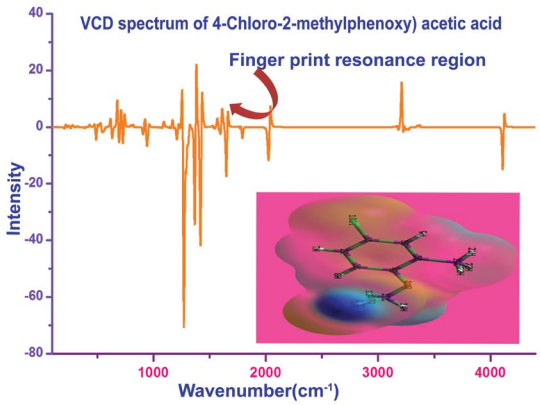

Figure 10) *VCD spectra of 4-Chloro-2-methylphenoxy) acetic acid*

injected to the base along with methyl group, the Antimicro-bioactivity is progressively induced in the compound. This type chemical activity change can be measured by ECT value of the compound. Here, this value of the compound in IR and UV-visible region were 2.155 and 2.153 respectively whereas the value of the base was 1.92. Therefore, this increment of ECT showed the enriched chemical activity of the substituted compound.

Polarization and hyper polarization activity

The first order and second order polarization is usually induced by the displacement of charge domains with respect to chemical equilibrium forces existed during the formation of the compound. Such kind of charge cloud orientation is synchronized by and π- bonding interactions taking place among molecular site and this charge displacements created strong multi dipole moments. The net dipole moments are making hypo and hyper activity within the compositional entities which mainly renovate the objective chemical activity in the compounds. The first order and second order functional Polarizability and first order hyperpolarizability scale was depicted in Table 8.

The designed average Polarizability and anisotropy of the Polarizability of 4-Chloro-2-methylphenoxy acetic acid was determined and were 163 × 10^{-30} esu and 227 × 10^{-30} esu respectively and the hyperpolarizability (β) was found to be 275 × 10^{-30} esu. According to the literature (17), the observed values of hypo polarization activity was found to be well above the drug activity region

TABLE 8

The dipole moments μ (D), the polarizability α(a.u.), the average polarizability αo (esu), the anisotropy the polarizabilityΔα(esu),and the first hyperpolarizability β(esu) of (4-Chloro-2-methylphenoxy) acetic acid

Parameter	a.u.	Parameter	a.u.
α_{xx}	-89.7872	β_{xxx}	23.322
α_{xy}	1.9883	β_{xxy}	37.086
α_{yy}	-80.8535	β_{xyy}	-14.49
α_{xz}	2.0741	β_{yyy}	4.7534
α_{yz}	-1.4261	β_{xxz}	16.609
α_{zz}	-79.2802	β_{xyz}	-14.01
α_{tot}	163.664	β_{yyz}	4.5288
Δα	227.229	β_{xzz}	29.086
μ_x	1.5627	β_{yzz}	-7.819
μ_y	1.3708	β_{zzz}	14.987
μ_z	0.3114	β_{tot}	275.68
Δμ	2.102		

and the present compound is able to be a novel drug. The hyper Polarizability of this compound found to be prominent level of drug activeness and tolerance of consistent drug potential. So this compound can be used as starting materials for advanced drug construction.

The partial polarization index was higher in xx and yy coordinates where the phenoxy and acid groups of chain was placed than other coordinates. The hyper polarization constant was identified very high in xxx and xxy and xzz coordinates. This view described that, the polarization path was preseted in coil structure which is very complicated arrangement by which the complex chemical property was instinctive.

NBMO transition analysis

The essential chemical potential of the aromatic system for causing peculiar drug property is not only stored in bonding orbitals and also non-bonding molecular orbitals (NBMO). The multiple classes of transitions between the non-bonded molecular energy levels are scaling the stored chemical energy and how many numbers of transitions contributing the prepared drug property. In NBMO, according to the selection rule, the transitions are promising in phase interaction orbital levels. These transition levels are listed in Table 9.

In this case, several electronic transitions were identified between available electron concentration zone to unfilled energy state from which the protected chemical energy swap (transitions) between important entities causing key medicinal property has been predicted and thereby augmented. In the primary case, within the six membered ring, the energy of 3.73 and 3.00 kcal/mol were transferred from C1-C2 to C1-C6 and C2-C3 respectively which were assigned as π - π * interaction system. Similarly, the 16.41 and 19.06 kcal/mol amount of energy were identified to transfer from C1-C2 to C3-C4 and C5-C6 respectively. Such amount of energy was very high and was found to be transferred already from acetic acid chain; this energy was harvested during these transitions.

The important transitions have been observed from C3-C4 to C1-C2 and C5-C6 by consuming 21.3 and 17.9 kcal/mol. energy with difference of kubo gap 0.30 a.u with occupancy value of 1.97. This energy was rather same which was observed in reverse order in previous case. Another transition within the ring was appeared from C5-C6 to C1-C2 and C3-C4 by consuming energy of 19.9 and 20.89 kcal/mol. From these transitions among * π - π * interaction systems, it was confer that, the stacking electronic energy within the ring which was transferred from chain was oscillated and thus the resultant chemical property was achieved.

Usually, the energy was transferred unidirectional from ligand to ring which was evidenced in this case by observing the transition from Cl10 to C1-C2 of ring system which was assigned within - * interaction system. At particular state of transition systems, the maximum energy absorption is taking place which would be the saturated electronic energy for generating desired property. This energy of 167.7 and 226.9 kcal/mol were identified at C1-C2 and C3-C4 to C5-C6 in * and π-π* interactive system. Finally, it was concluded that, the exchange electronic energy for this complex system to produce biological activity were identified and recognized which are observed to be finitely confined between ring and ligand species.

TABLE 9

The calculated NBO of (4-Chloro-2-methylphenoxy) acetic acid by second order Perturbation theory

Donor (i)	Type of bond	Occupancy	Acceptor (j)	Type of bond	E2 kcal/ mol	Ej – Ei au	F(lj) au
C1-C2	π	1.98543	C1-C6	π*	3.73	1.3	0.039
	π	1.98543	C2-C3	π*	3	1.3	0.033
	π	1.98543	C3-C4	π*	16.41	1.29	0.033
C1-C6	π	1.9763	C5-C6	π*	19.06	0.3	0.037
	σ	1.9763	C1-C2	σ*	3.75	1.3	0.053
	σ	1.95201	C5-C6	σ*	3.5	1.31	0.045
	σ	1.98003	C5-C19	σ*	3.28	1.14	0.032
C2-C3	σ	1.79936	C1-C2	σ*	3.64	1.28	0.028
	σ	1.79936	H8	σ*	5.3	0.85	0.037
C2-H7	σ	1.9884	C4-O11	σ*	4.7	1.04	0.033
	σ	1.9884	C1-C6	σ*	4.31	1.09	0.054
C3-C4	π	1.97473	C3-C3	π*	3.55	1.08	0.044
	π	1.97473	C4-C5	π*	4.89	1.27	0.041
	π	1.9793	C1-C2	π*	21.38	0.29	0.033
	π	1.9827	C5-C6	π*	17.94	0.3	0.035
C3-H8	σ	1.99627	C4-C5	σ*	3.97	1.09	0.029
C4-C5	σ	1.9767	C3-C4	σ*	4.4	1.26	0.047
C5-C6	π	1.9767	C1-C6	π*	3.98	1.27	0.054
C5-C6	π	1.99863	C1-Cl10	π*	4.67	0.85	0.151
	π	1.99863	C1-C2	π*	19.95	0.27	0.076
	π	1.99863	C3-C4	π*	20.89	0.27	0.122
C6-H9	σ	1.99863	C1-C2	σ*	4.24	1.1	0.142
C12-H14	σ	1.99863	C4-O11	σ*	3.74	0.88	0.081
	σ	1.99887	C15-O16	σ*	5.32	0.88	0.154
O17-H18	σ	1.99887	C12-C15	σ*	3.97	1.1	0.102
C19-H21	σ	1.99887	C4-C5	σ*	4.39	10.67	0.094
Cl10	σ	1.99887	C1-C2	σ*	11.9	10.43	0.092
O11	LP	1.99887	C3-C4	σ*	6.26	10.19	0.096
O11	LP	1.99869	C3-C4	σ*	27.18	11.07	0.158
	LP	1.99869	C12-H13	σ*	4.54	0.69	0.069
	LP	1.99869	C12-C15	σ*	8.47	0.66	0.115
O16	LP	1.99869	C15	LP	17.26	1.72	0.082
	LP	1.99869	C12-C15	σ*	18.97	0.62	0.096
	LP	1.99869	C15-O17	σ*	32.5	0.63	0.072
O17	LP	1.99858	C15-O16	σ*	6.96	1.22	0.139
	LP	1.99858	C15-O16	σ*	41.4	0.38	0.101
C1-C2	σ	1.99858	C5-C6	σ*	167.75	0.02	0.085
C3-C4	σ	1.99858	C5-C6	π*	226.9	10.75	0.128
C15-O16	σ	1.99858	C15-O16	σ*	4.54	0.56	0.119
	LP	1.99895	C6	LP	2.08	10.92	0.134
CL 10	LP	1.99884	C1-CL 10	σ*	0.68	10.19	0.075
Cl 10	LP	2	C1	LP	1.76	11.35	0.126
	LP	2	C1	LP	0.57	11.34	0.072
O11	LP	2	C1	LP	0.6	11.83	0.075
	LP	1.99976	C4	LP	1.4	20.05	0.15
C12	LP	1.99976	C12	LP	0.53	19.91	0.092
	LP	1.99894	C15	LP	0.51	11.64	0.069
	LP	1.99894	C4-O11	σ*	0.98	10.42	0.091
	LP	1.99894	O11-C12	σ*	1.07	10.4	0.095
	LP	1.99894	C15-O17	σ*	0.57	10.32	0.07
C15	LP	1.99946	C15-O17	σ*	1.1	10.45	0.099
O16	LP	1.99976	C15	LP	7.12	19.66	0.336
O17	LP	1.9997	C3-H8	σ*	9.62	19.65	0.405

VCD profile

The simulated VCD spectrum for tailored structure was exhibited in the Figure 10. The symmetrical pattern of the chirality of the compound could be identified from sequential form of absorption and transmission of energy by optimized molecular structure. Such pattern embedded with wavenumber of IR region recognize the presence of toxicity and thereby comfortable to explain whether the compound is biologically and pharmaceutically active Usually, the symmetrical sequence in finger print as well as substitution

region of the spectrum represents the background of the toxicity induction (49). Here, the observed signals at sequential pattern between absorption and transmission were found to be differed ±0.09 identified in the VCD spectrum. Therefore, the title compound having series VCD pattern which leads to contain veiled toxic effect which conferred that, the compound itself would be the simple drug as well as starting material for drug production with distended chemical clarity.

CONCLUSION

The structural, biological and physico-chemical properties of (4-Chloro-2-methylphenoxy) acetic acid have been thoroughly studied using corresponding parameters observed from experimental tools and computed from computational tools. Both obtained results emphasized the drug activity of the present compound and the following conclusions were observed.

- The molecular geometry deformation showed the distortion of hexagonal structure which described the distortion of basic property of the ring and existence of new property.
- From the arrangement of molecular charge intensity in mulliken charge levels, it was clear that, the necessary electronic content of energy was moved from OCH_2COOH chain and Cl to the hexagonal ring, which created the asymmetric charge equilibrium and it was controlled and regulated by methyl group on head of the ring. This view of wide dispersal charge entities in the compound produced antibiotic nature.
- From the RO5 rules, it was inferred that, the present drug is suitable for oral formulations and based on the obtained results of biological parameters, the present drug was largely free of toxic effects.
- From the C-H vibrational analysis, it was clear that, the C-H bending vibrations were found to be well within their limited array and it is also conclude that, energy of C-H bonds were affected in higher region than lower region.
- The entire OH vibrations significantly discussed and the locations of the peaks were keenly monitored. From this discussion, it was infer that, from the elevated vibrations, it was confirmed that, the chemical potential concentrated over COOH for generating enriched antibiotic property.
- The NMR examinations clear that, the charge cloud was moved disproportionately flow from methyl and chlorine to ring and ring to acetic acid ligand via nodal site of carbons in the ring. In this way, the exchange of electronic potential taking place between ring and ligands and generating consistent drug property such as antibiotic potential.
- From this interaction profile of FMP, it was conferred that, the π and bonding interaction orbital domains available in ring and chain for the charge cloud orientation to drift chemical energy among intra molecular electronic entities to induce the strong chemical potential to persuade drug property.
- From CT complex analysis, it was conferred that, the exchange electronic energy for this complex system to produce biological activity were identified and recognized which are observed to be finitely confined between ring and ligand species.
- The title compound having series VCD pattern which leads to contain veiled toxic effect which conferred that, the compound itself would be the simple drug as well as starting material for drug production with distended chemical clarity.

REFERENCES

1. Gurumurthy R, Sathiyanarayanan KI, Gopalakrishnan M. Kinetics and mechanism of oxidation of ethyl phenylthioacetates by bromamine-B. Bull Chem Soc Jpn. 1992;65(4):1096-100.
2. Karthikeyan B, Gurumurthy R, Gopalakrishnan M, et al. Asian Chem Lett. 1998;97:2-3.
3. Timchalk C. Comparative inter-species pharmacokinetics of phenoxyacetic acid herbicides and related organic acids: evidence that the dog is not a relevant species for evaluation of human health risk. Toxicology. 2004;200(1):1-9.
4. Sundaraganesan N, Meganathan C, Karthikeyan B. FT-IR, FT-Raman spectra and quantum chemical calculations of some chloro substituted phenoxy acetic acids. Spectrochim. Acta A 2008;70(2):430-8.
5. Cserhati T, Forgacs E. Phenoxyacetic acids: separation and quantitative determination. J Chromatogr B Biomed Sci Appl. 1998;717(1-2):157-78.
6. Crafts AS. The chemistry and mode of action of herbicides: Y AS Crafts. Interscience publishers; 1961.
7. Kohn W, Sham LJ. Self-consistent equations including exchange and correlation effects. Phys Rev 1965;140(4A):A1133.
8. Sarac S, Safak C, Erdogan H, et al. Substitute d phenoxyacetic acid derivatives and their antimicrobial activities. Pharm Sci Exp Pharmacol. 1991;11:1-1.
9. Kociba RJ, Keyes DG, Lisowe RW, et al. Results of a two-year chronic toxicity and oncogenic study of rats ingesting diets containing 2, 4, 5-trichlorophenoxyacetic acid (2, 4, 5-T). Food Chem Toxicol.1979;17(3):205-21.
10. Smith FA, Murray FJ, John JA, et al. Three-generation reproduction study of rats ingesting 2, 4, 5-trichlorophenoxyacetic acid in the diet. Food Chem Toxicol. 1981;19:41-5.
11. Vijay Kumar S, Rao LM. (4-Chlorophenoxy) acetic acid. Acta Crystallographica Section B: Structural Crystallography and Crystal Chemistry. 1982;38(7):2062-4.
12. Karthikeyan B, Saravanan B. Raman spectral analysis of phenoxyacetic acid and some chloro substituted phenoxyacetic acids. Spectrochimica Acta Part A: Molecular and Biomolecular Spectroscopy. 2006;63(3):619-23.
13. Madanagopal A, Periandy S, Gayathri P, et al. Molecular structure activity on pharmaceutical applications of Phenacetin using spectroscopic investigation. J Mol Struct. 2017;1127:611-25.
14. Moorthy N, Prabakar PCJ, Ramalingam S, et al. Spectroscopic analysis, AIM, NLO and VCD investigations of acetaldehyde thiosemicarbazone using quantum mechanical simulations. J Phys Chem Solids.2016;95:74-88.
15. Moorthy N, Prabakar PCJ, Ramalingam S, et al. Vibrational, NMR and UV-visible spectroscopic investigation and NLO studies on benzaldehyde thiosemicarbazone using computational calculations. J Phys Chem Solids.2016;91:55-68.
16. Xavier S, Periandy S. Spectroscopic (FT-IR, FT-Raman, UV and NMR) investigation on 1-phenyl-2-nitropropene by quantum computational calculations. Spectrochim Acta A Part A: Molecular and Biomolecular Spectroscopy. 2015;149:216-30.
17. Aarthi R, Ramalingam S, Periandy S, et al. Molecular structure-associated pharmacodynamic investigation on benzoyl peroxide using spectroscopic and quantum computational tools. J Taibah Univ Sci.2018;1-19.
18. Lipinski CA, Lombardo F, Dominy BW, et al. Experimental and computational approaches to estimate solubility and permeability in drug discovery and development settings. Adv Drug Deliv Rev. 1997;23(1-3):3-25.
19. Lipinski CA. 6 Methods. Pharmacol Toxicol.2000;87(s3):17-17.
20. Hopkins AL, Groom CR. The druggable genome. Nat Rev Drug Discov. 2002;1(9):727-30.
21. Keserü GM, Makara GM. The influence of lead discovery strategies on the properties of drug candidates. Nat Rev Drug Discov. 2009;8(3):203-12.
22. Alexander SP, Christopoulos A, Davenport AP, et al. The Concise guide to pharmacology 2017/18: G protein-coupled receptors. Br J Pharmacol.2017;174:S17-S129.
23. Gronemeyer H, Gustafsson J-Å, Laudet V. Principles for modulation of the nuclear receptor superfamily. Nat Rev Drug
24. Socrates G. Infrared and raman characteristic group frequencies: Tables and Charts. (3rd ed). J. Wiley and Sons: Chichester.2001;Xviii:348.
25. Smith W. Infrared spectroscopy W. O. George and P. S. McIntyre, Wiley, Chichester, 1987:537.
26. Krishnakumar V, Prabavathi N. Simulation of IR and Raman spectral based on scaled DFT force fields: A case study of 2-amino 4-hydroxy 6-trifluoromethylpyrimidine, with emphasis on band assignment. Spectrochim Acta A Part A: Molecular and Biomolecular Spectroscopy. 2008;71(2):449-57.

27. Altun A, Gölcük K, Kumru M. Structure and vibrational spectra of p-methylaniline: Hartree-Fock, MP2 and density functional theory studies. J Mol Struct:Theochem.2003;637(1-3):155-69.
28. Pandey SM, Singh SJ. Electronic absorption-spectra of ortho-bromobenzonitrile in vapor-phase. Indian J Pure Appl Phys. 1976;14(7):300-4.
29. Sun YX, Hao QL, Yu ZX, et al. Experimental and theoretical studies on vibrational spectra of 4-(2-furanylmethyleneamino) antipyrine, 4-benzylideneaminoantipyrine and 4-cinnamilideneaminoantipyrine. Spectrochim Acta A Part A: Molecular and Biomolecular Spectroscopy.2009;73(5):892-901.
30. Krishnakumar V, Xavier RJ. Normal coordinate analysis of vibrational spectra of 2-methylindoline and 5-hydroxyindane.
31. Karabacak M, Karagöz D, Kurt M. FT-IR, FT-Raman vibrational spectra and molecular structure investigation of 2-chloro-4-methylaniline: A combined experimental and theoretical study. Spectrochim Acta A Part A: Molecular and Biomolecular Spectroscopy. 2009;72(5):1076-83.
32. Green JH, Harrison DJ, Stockley CP. Vibrational spectra of pentachlorophenol and pentachlorothiophenol. J Mol Struct. 1976;33(2):307-14.
33. Abdel-Shafy H, Perlmutter H, Kimmel H. Vibrational studies of monosubstituted halogenated pyridines. J Mol Struct.1977;42:37-49.
34. Sajan D, Binoy J, Pradeep B, et al. NIR-FT Raman and infrared spectra and ab initio computations of glycinium oxalate. Spectrochim Acta A Part A: Molecular and Biomolecular Spectroscopy. 2004;60(1-2):173-80.
35. Furić K, Mohaček V, Bonifačić M, et al. Raman spectroscopic study of H_2O and D_2O water solutions of glycine. J Mol Struct.1992;267:39-44.
36. Dollish FR, Fateley WG, Bentley FF. Characteristic Raman Frequencies of organic compounds. Analytica Chimica Acta. 1975;75(2):492.
37. Wiberg KB, Shrake A. A vibrational study of cyclohexane and some of its isotopic derivatives-III. A vibrational analysis of cyclohexane, cyclohexane-d12, cyclohexane-1,1,4,4-d4 and cyclohexane-1,1,2,2,4,4,5,5-d8. Spectrochim Acta Part A: Molecular Spectroscopy. 1973;29(3):583-94.
38. Bahgat K, Al-Den Jasem Na, El-Emary T. Theoretical and experimental investigations on the structure and vibrational spectra of 6-amino-3-methyl-1-phenyl-1H-pyrazolo-[3,4-b] pyridine-5-carboxylic acid and 6, 7-dihydro-3-methyl-6--oxo-1-phenyl-1H-pyrazolo [3,4-b] pyridine-5-carbonitrile. J Serb Chem Soc. 2009;74:555-71.
39. Green JHS, Harrison DJ, Kynaston W. Vibrational spectra of benzene derivatives—XII 1,2,4-trisubstituted compounds. Spectrochim Acta Part A: Molecular Spectroscopy. 1971;27(6):807-15
40. Ramalingam S, Periandy S, Karabacak M, et al. Spectroscopic (FT-IR/FT-Raman) and computational (HF/DFT) investigation and HOMO/LUMO/MEP analysis on 2-amino-4-chlorophenol. Spectrochim Acta Part A: Molecular and Bimolecular Spectroscopy. 2013;104:337-51.
41. Koegel RJ, Greenstein JP, Winitz M, et al. Studies on Diastereoisomeric α-amino acids and corresponding α-Hydroxy Acids: V Infrared Spectra. J Am Chem. Soc.1955;77(21):5708-20.
42. Koczon P, Baranska H, Lewandowski W. Asian Journal of Physics, 3 (1994) 71-79.
43. Oki M, Hirota M. Intramolecular Hydrogen bonding in α-Keto-and α-Alkoxy-carboxylic Acids. VI. Substituent Effects on the Energy of the Hydrogen Bonding in α-Alkoxy-and α-Aryloxyacetic Acids. Bull Chem Soc Jpn. 1963;36(3):290-6.
44. Sathyanarayana DN. Vibrational spectroscopy: theory and applications. New Age International; 2015.
45. Ahmad S, Mathew S, Verma PK. Laser Raman and FT-infrared spectra of 3, 5-dinitrobenzoic acid. Indian J Pure Appl Phys.1992;30(12):764-5.
46. Mulliken RS. Molecular compounds and their spectra. III. The interaction of electron donors and acceptors. J Phys Chem. 1952;56(7):801-22.
47. Bohacek RS, McMartin C. Definition and display of steric, hydrophobic, and hydrogen bonding properties of ligand binding sites in proteins using Lee and Richards accessible surface: validation of a high-resolution graphical tool for drug design. J Med Chem.1992;35(10):1671-84.
48. Tro NJ, Fridgen T, Shaw L. Chemistry: A Molecular Approach, 2e.
49. Stephens PJ, Devlin FJ, Cheeseman JR. VCD spectroscopy for organic chemists. CRC Press; 2012:25.